Canopy1, a positive feedback regulator of FGF signaling, controls progenitor cell clustering during Kupffer's vesicle organogenesis

Takaaki Matsui[1*], Siripong Thitamadee[1], Tomoko Murata[1], Hisaya Kakinuma[2], Takuji Nabetani[3], Yoshio Hirabayashi[3], Yoshikazu Hirate[4], Hitoshi Okamoto[2], and Yasumasa Bessho[1]

[1]Gene Regulation Research, Graduate School of Biological Sciences, Nara Institute of Science and Technology, 8916-5 Takayama, Nara 630-0101; [2]Laboratory for Developmental Gene Regulation, Brain Science Institute, RIKEN, 2-1 Hirosawa, Wako, Saitama 351-0198; [3]Hirabayashi Research Unit, Brain Science Institute, RIKEN, Wako, Saitama 351-0198; [4] Department of Cell Fate Control, Institute of Molecular Embryology and Genetics, Kumamoto University, 2-2-1 Honjo, Kumamoto 860-0811, Japan.

Key words: Cell cluster formation; Left-right patterning; Canopy; Positive feedback loop

Running title: Regulation of DFC clustering by Cnpy1

* Corresponding author

E-mail: matsui@bs.naist.jp

Tel: +81-743-72-5507

Fax: +81-743-72-5479

Abstract

The assembly of progenitor cells is a crucial step for organ formation during vertebrate development. Kupffer's vesicle (KV) is a key organ required for the left-right asymmetric body plan in zebrafish, and is generated from a cluster of approximately 20 dorsal forerunner cells (DFCs). Although several genes are known to be involved in KV formation, how DFC clustering is regulated and how cluster formation then contributes to KV formation remain unclear. Here we show that positive feedback regulation of FGF signaling by Canopy1 (Cnpy1) controls DFC clustering without affecting DFC specification and DFC number. Cnpy1 positively regulates FGF signals within DFCs, which in turn promotes Cadherin1-mediated cell adhesion between adjacent DFCs to sustain cell cluster formation. When this FGF positive feedback loop is disrupted, the DFC cluster fails to form, eventually leading to KV malformation and defects in the establishment of laterality. Our results therefore uncover both a previously unidentified role of FGF signaling during vertebrate organogenesis and a regulatory mechanism underlying cell cluster formation, which is an indispensable step for formation of a functional KV and establishment of the left-right asymmetric body plan.

~~¥~~body

Introduction

Fibroblast growth factor (FGF) signaling plays crucial roles in multiple morphogenetic processes of vertebrate development including gastrulation movement, mesoderm formation and left-right (LR) patterning (1-3). Since gain- or loss-of-function of FGF signaling results in morphological changes in the embryo, some mechanism must ensure appropriate FGF signal levels in space and time for proper morphogenesis throughout development. FGF effectors acting as positive or negative regulators show a wide range of expression patterns and activities, which contributes to the precise regulation of FGF signal activity (1, 4). Although most effectors identified to date act as negative regulators of FGF signaling, a few that positively regulate FGF activity have been reported (1, 4).

We recently identified a positive regulator of FGF signaling in zebrafish named *canopy1* (*cnpy1*), which is required for maintenance of the midbrain-hindbrain boundary (MHB) (5). Expression of *cnpy1* was restricted to the MHB at late-somitogenesis stages, whereas *cnpy1* was broadly distributed in earlier embryos (ref. 5 and Fig. S1A), suggesting an additional role(s) for Cnpy1-mediated FGF signaling beyond the regulation of MHB formation. In this study, we characterize *cnpy1* in detail during early zebrafish development, and show that a Cnpy1-mediated positive feedback loop of FGF signaling promotes cell cluster formation between dorsal forerunner cells (DFCs) during gastrulation. We also demonstrate that the failure of DFCs to cluster

when this FGF positive loop is disrupted eventually leads to Kupffer’s vesicle (KV) malformation and randomization of LR asymmetric patterning. Hence, our results uncover the signaling mechanism for DFC clustering, which is prerequisite for KV formation and LR asymmetric patterning in zebrafish.

Results

Positive feedback loop of FGF signaling mediated by Cnpy1 is activated specifically in DFCs during zebrafish gastrulation

To reveal the role of Cnpy1-mediated FGF signaling in early zebrafish embryos, we first looked for the specific regions and cells in which Cnpy1 positively regulates FGF signaling, by monitoring FGF signal activity using an anti-di-phosphorylated Erk (dp-Erk) antibody. FGF signal activity was observed in the blastoderm margin and DFCs at mid-gastrulation (Fig. S2A), whereas knockdown of *cnpy1* with an antisense morpholino (*cnpy1*-MO) reduced the FGF activity in DFCs (Fig. S2B). To test whether Cnpy1 is required autonomously for the FGF activation in DFCs, we next knocked down *cnpy1* in DFCs but not in the rest of the embryo using a DFC-specific MO delivery method (6-8). Similar to *cnpy1* morphants, DFC-specific knockdown of *cnpy1* ($\mathrm{DFC}^{\mathit{cnpy1}\text{-MO}}$) reduced the FGF activity in DFCs (Fig. 1B and Fig. S2C). Since *cnpy1* expression is induced by Fgf8 in the MHB (5), we checked whether FGF signaling is also required for *cnpy1* expression in DFCs. We found that *cnpy1* expression in DFCs could indeed be blocked by knockdown of *fgf8* (Fig. S2G) or by treatment with the FGF receptor inhibitor SU5402 (Fig. 1D). These results imply that a positive feedback loop between FGF and Cnpy1 is activated specifically in DFCs at mid-gastrulation.

Cnpy1 function within DFCs is required for DFC clustering

DFCs are progenitor cells of Kupffer's vesicle (KV), which is a key organ required for LR patterning in zebrafish (9-11). At mid-gastrulation, a cluster of approximately 20

DFCs appears adjacent to the embryonic shield (12, 13). The DFC cluster then moves, in contact with the overlying surface epithelium, to the vegetal pole and forms a more compact and oval-shaped cluster by late gastrulation (7, 11, 14). At the end of gastrulation, DFCs differentiate into ciliated epithelial cells of the KV, which generates the nodal flow required for the LR asymmetric body plan (7, 12, 13). Recent studies have shown that FGF signaling is required for morphogenesis and ciliogenesis of the KV and for LR patterning (2, 8, 15). Although knockdown of the FGF target genes *ier2* and *fibp1* is known to interfere with DFC formation (15), the contribution of FGF signaling prior to KV formation is poorly understood.

To investigate the morphogenetic role of Cnpy1 in DFC/KV formation, we analyzed the expression of markers specific for DFC fate specification (*sox32*) or differentiation (*no tail*) in *cnpy1*-MO-injected embryos. We found that the DFC cluster was broken up into multiple groups of cells (Fig. 1K and Fig. S3B, C, E), and the broad distribution of endoderm cells marked by *sox32* was disrupted (Fig. S3B), in *cnpy1* morphants. Even though *cnpy1* morphants showed a failure of DFC clustering, neither cell fate specification nor total cell number in DFCs was affected by *cnpy1* knockdown (Fig. S3B and Table S1). Similar to *cnpy1* morphants, DFC-specific knockdown of *cnpy1* resulted in a broken-up DFC phenotype, whereas DFC specification and cell number were unaffected (Fig. 1F, K, Fig.S3C, G and Table S1). When embryos were co-injected with *cnpy1*-MO and MO-resistant *cnpy1* mRNA ($\mathrm{DFC}^{\textit{cnpy1}\text{-MO+Cnpy1}}$), the broken-up DFC phenotype was significantly rescued (53%; $P = 0.00174$, Fig. 1I-K). Because, in the DFC-specific MO delivery method, the MO is also delivered to the yolk and the yolk syncytial layer (YSL), it was possible that effects of *cnpy1* in yolk/YSL might be essential for DFC clustering. To address this, we knocked down *cnpy1* in yolk/YSL but not in DFCs (yolk$^{\mathit{cnpy1}\text{-MO}}$), and found no DFC defects in terms of specification, cell number or cluster formation (Fig. 1H, K and Table S1). Live confocal imaging revealed that the sparse DFC populations in DFC$^{\mathit{cnpy1}\text{-MO}}$ embryos never assembled into a compact cluster, although normal downward migration was observed (Fig. S4F-J and Movie S2), indicating that Cnpy1 regulates formation of the cell cluster itself, rather than controlling directed cell migration. These results suggest that Cnpy1 is the factor, downstream of FGF signaling, which is required for cluster formation of DFCs in zebrafish embryos.

Cnpy1 function within DFCs is essential for KV ciliogenesis and LR patterning

Observation of DFCs using *Tg[sox17:GFP]* zebrafish embryos revealed that broken-up DFC phenotypes did not generate multiple clusters at the end of gastrulation. In DFC$^{\mathit{cnpy1}\text{-MO}}$-injected embryos, a rosette-like structure containing small a number of DFCs was formed, around which fragmented GFP signals that might signify dead cells could be observed, whereas a proper rosette structure containing a larger number of DFCs was evident in DFC$^{\text{control-MO}}$ embryos (Fig. S5C-E). These results suggest that the broken-up DFC clusters seen in DFC$^{\mathit{cnpy1}\text{-MO}}$ embryos reflect a failure in the recruitment of DFCs to the KV.

To examine how the failure of DFC cluster formation influences KV organogenesis and function, we investigated the presence and characteristics of primary cilia in the KV in DFC$^{cnpy1\text{-MO}}$ morphants using an anti-acetylated tubulin (A-tubulin) antibody. DFC-specific knockdown of *cnpy1* resulted in 60% and 35% reductions in the number and length, respectively, of primary cilia in the KV at early somitogenesis (Fig. 2B, C). As well as this disruption of ciliogenesis, lumen formation in the KV was incomplete (Fig. 2B'), suggesting that Cnpy1-mediated DFC clustering is required for proper formation of the KV. This idea is supported by the observation that the horseshoe-shaped pattern of *charon* expression in the caudal region of the KV was lost in DFC$^{cnpy1\text{-MO}}$ morphants (Fig. S6B, C). Consistent with the defects in DFC clustering, ciliogenesis and KV structure, knockdown of *cnpy1* altered the left-sided expression of *southpaw* (*spaw*) in the lateral plate mesoderm at late somitogenesis (Fig. S6E, F), and led to defects in cardiac laterality at later stages (Fig. 2E, F). Defective ciliogenesis and cardiac laterality in DFC$^{cnpy1\text{-MO}}$ embryos could be rescued by co-injection of MO-resistant *cnpy1* mRNA (Fig. 2C and Fig. S7D). Collectively, these results suggest essential roles for *cnpy1* in KV ciliogenesis and the LR asymmetric body plan.

Amplification of FGF signaling by Cnpy1 is required for DFC cluster formation

The above phenotypes in DFC$^{cnpy1\text{-MO}}$ embryos are reminiscent of the defects seen in embryos in which FGF signaling has been disrupted, such as *fgf8*, *fgfr1*, *ier2* and *fibp1* morphants (Fig. 2F, Fig. S6F; see also ref. 8, 15). To test for a functional relationship between FGF signaling and *cnpy1* in DFC clustering, we analyzed whether the loss of

FGF signaling function could phenocopy *cnpy1* morphants. Intriguingly, *ace/fgf8* mutations lead to failures of KV formation and LR patterning (2). While *fgf8* is expressed in and around DFCs (2), overlapping with *cnpy1* expression, the role of *fgf8* in DFC clustering is uncertain. We therefore examined the contribution of *fgf8* to the formation of the DFC cluster. As did *cnpy1*-MO-injected embryos, *fgf8* morphants exhibited the broken-up DFC phenotype but normal DFC specification and cell number (Fig. 3A-C and Table S1). *fgf8* knockdown also resulted in defects in KV formation (Fig. S6C) and LR patterning (Fig. 2F and Fig. S6F). We also found that 57% of the *ace/fgf8* mutants displayed the broken-up DFC phenotype (Fig. S8C, D). These results suggest that *fgf8* plays an essential role in DFC clustering and that Cnpy1 contributes to this role.

We have shown that Cnpy1 is an endoplasmic reticulum (ER)-localized protein that can interact with Fgfr1 (5). However, it is still unclear how Cnpy1 modulates FGF signaling. As the ER is a quality-control system that ensures maturation of secreted and membrane-bound proteins (16, 17), we reasoned that Cnpy1 might assist in the maturation of Fgfr1 in the ER, and tested this using *in vitro* glycosylation assays (for details, see Materials and Methods in SI Appendix). Mature forms of Fgfr1 increased up to two-fold in Cnpy1-overexpressing cells (Fig. 4A, B), suggesting that Cnpy1 enhances FGF signaling by promoting the maturation of its receptor in the ER. This idea was further supported by proteomic data showing that a human Cnpy1 homolog binds to ER chaperones and folding-assisting enzymes (Table S2).

If the amplification of FGF signals via Cnpy1-mediated Fgfr1 maturation is required for DFC clustering, it seemed possible that forced activation of Fgfr1 would restore the failure of DFC clustering in DFC$^{cnpy1\text{-MO}}$ embryos. Using iFGFR1, a conditional activation system for Fgfr1 that depends on AP20187-induced dimerization (5, 18), we activated Fgfr1 spatially and temporally in DFCs (for details, see Materials and Methods in SI Appendix). AP20187-mediated conditional activation of Fgfr1 in DFCs led to a 67% reduction in the broken-up DFC phenotype relative to vehicle (ethanol)-treated controls ($P = 2.89 \times 10^{-4}$; Fig. 3D-F). Despite the conditional activation being restricted to DFCs during gastrulation, this manipulation partially restored deficiencies in cilium number ($P = 9.23 \times 10^{-3}$) and length ($P = 7.77 \times 10^{-3}$) in the KV (Fig. 3G-J) and of cardiac laterality at later stages ($P = 0.0114$; Fig. 3K). These results therefore indicate that Cnpy1 function reinforces FGF signal activity within DFCs, and suggest that DFC clustering mediated by this positive loop is prerequisite for formation of a functional KV and proper LR patterning.

Induction of *cdh1* by Cnpy1-mediated FGF signaling is responsible for generating cell adhesion between DFCs during cell cluster formation

To investigate the cellular function of Cnpy1 in DFC clustering, we analyzed cytoskeletal organization in DFCs of DFC$^{cnpy1\text{-MO}}$ embryos. Phalloidin staining showed that F-actin accumulated to a high level at the cell-cell contact sites between DFCs containing control-MO (Fig. S9A), meaning that DFCs adhered tightly to each other in control embryos. In contrast, cell-cell adhesion between DFCs containing *cnpy1*-MO, evaluated by F-actin accumulation, was weaker than that between control-MO-containing DFCs (Fig. S9B). These results suggest that Cnpy1-mediated FGF signaling modulates cell adhesions between DFCs during the control of cell clustering.

Recent studies have shown that the T-box transcription factor Tbx16 regulates DFC/KV formation in a cell-autonomous manner, although the underlying mechanism is still unclear (7). Tbx16 is also a mediator of FGF signaling, a function that is implicated in the control of cell adhesions via the transcriptional regulation of *paraxial protocadherin* (*papc*) (7, 19). Although *papc* expression is not detected in DFCs, *cadherin1* (*cdh1*) expression is (7, 20); we thus hypothesized that *tbx16* and *cdh1* are downstream effectors of FGF signaling during the control of DFC clustering. To test this possibility, we analyzed whether Cnpy1-mediated FGF signaling affects expression of *tbx16* or *cdh1* within DFCs. DFC$^{\textit{cnpy1}\text{-MO}}$ embryos showed reduced *tbx16* or *cdh1* expression in sparse DFC populations (Fig. 5B, D and Fig. S10B, D). Importantly, DFC-specific knockdown of *tbx16* (DFC$^{\textit{tbx16}\text{-MO}}$) also led to a reduction of *cdh1* expression within DFCs (Fig. S10E, G), suggesting that *tbx16* plays an important role in *cdh1* expression within DFCs.

We next investigated whether DFC-specific knockdown of *tbx16* (DFC$^{\textit{tbx16}\text{-MO}}$) or *cdh1* (DFC$^{\textit{cdh1}\text{-MO}}$) could phenocopy DFC$^{\textit{cnpy1}\text{-MO}}$ morphants. DFC-specific knockdown of either *tbx16* or *cdh1* led to the broken-up DFC phenotype but not to failures of DFC specification or cell number (Fig. S11B, C, D and Table S1), outcomes similar to those observed in DFC$^{\textit{cnpy1}\text{-MO}}$ morphants. These results suggested that a genetic cascade including *tbx16* and *cdh1* mediates FGF signal-dependent DFC clustering, and prompted us to examine whether the broken-up DFC phenotype in DFC$^{\textit{cnpy1}\text{-MO}}$ embryos could be rescued by overexpressing Cdh1. This restored DFC clustering in 60% of the manipulated embryos, relative to overexpression of mRFP as a control (Fig. 5E-G). Hence, our results demonstrate that the Cnpy1-mediated FGF positive feedback loop regulates *tbx16* and *cdh1* to assemble cells into a tight cluster.

Taking these results together, we propose the following stepwise regulatory mechanism underlying DFC cluster formation (Fig. 5H). First, FGF signaling is initiated in DFCs by Fgf8. Second, the up-regulated Cnpy1 within DFCs modulates FGF signal strength by enhancing Fgfr1 maturation in the ER. Third, the amplified FGF signals then promote cell-cell adhesion between adjacent DFCs through the action of Cdh1, eventually leading to the generation of a tight and stable cluster of DFCs.

Discussion

Cell signaling is required for controlling vertebrate development. Characterization of positive or negative regulators, which contribute to the precise regulation of signal activity, enables us to understand signal mechanisms underlying multiple processes of embryonic development. In this study, we characterize a positive FGF regulator named Canopy1 and show a previously unidentified role of FGF signaling during zebrafish development. In addition, we provide specific insights into the molecular and cellular mechanisms linking FGF signaling, DFC clustering, KV formation and the LR asymmetric body plan.

An earlier contribution of FGF signaling to left-right asymmetric body plan

Accumulated evidence points to crucial roles of FGF signaling in several processes of LR asymmetric patterning (2, 8, 9, 15, 21, 22). Two recent studies, in particular, have shown that FGF signaling regulates KV ciliogenesis during LR pattering (8, 15). However, we uncover the importance of this signal pathway for the regulation of progenitor cell clustering at a stage prior to KV ciliogenesis: DFC-specific knockdown of *cnpy1*, *tbx16* or *cdh1* results in broken-up DFC clusters during gastrulation. The cause of such a discrepancy may originate from the differences of regulatory mechanisms underlying DFC cluster formation and ciliogenesis. DFC clustering requires activities of FGF-dependent effectors such as *tbx16* and *cdh1*, as shown in this study. In contrast, ciliogenesis depends on the intraflagellar transport pathway regulated by the coordinated action of various signals including FGF, Sonic hedgehog, and/or Wnt pathways (8, 15, 24, 25).

In this study, we have proposed that Cnpy1 controls DFC clustering, KV formation and ciliogenesis by promoting Fgfr1 maturation. However, Neugebauer et al. showed a different and specific role of *fgfr1* in ciliogenesis and KV formation: DFC-specific knockdown of *fgfr1* (DFC$^{\textit{fgfr1}\text{-MO}}$) leads to short cilia without affecting cilium number and KV size (8). This discrepancy may explain the redundant action between *fgfr1* paralogs. A recent study has shown that the *fgfr1* which was knocked down by Neugebauer et al. (8) and a second *fgfr1* (*fgfr1b*) can functionally compensate for each other during early development (23). We reasoned that DFC-specific knockdown of *cnpy1* might lead to defects severer than those seen in DFC$^{\textit{fgfr1}\text{-MO}}$ embryos because Cnpy1 can modulate the maturation of both receptors within DFCs. To test this possibility, we used a dominant-negative form of Fgfr1 (dn-Fgfr1) which lacks the cytoplasmic domain and attempted to inhibit the functions of both receptors. Because injection of *dn-fgfr1* mRNA into one-cell embryos led to severe defects in mesoderm formation and axis elongation, as shown previously (1), we used DFC-specific gene transfer methods (see Materials and Methods in SI Appendix). As seen in DFC$^{\textit{cnpy1}\text{-MO}}$ embryos, DFC$^{\text{dn-Fgfr1}}$ embryos resulted in a broken-up DFC phenotype (Fig. S12B, C). Treatment with SU5402 (100 μg/ml) also led to broken-up DFC clusters (Fig. 1D). These results therefore suggest that strong loss-of-function effects on Fgfr1, such as *cnpy1* knockdown, dn-Fgfr1 overexpression and SU5402 treatment, prevent DFCs from organizing into a tight cell cluster, and that Cnpy1 may assist the maturation of both receptors within DFCs (see below). On the other hand, mild loss of Fgfr1 function including the single knockdown of *fgfr1* performed by Neugebauer et al. (8) may yield the specific defect in cilium length.

Our results do not support data showing that loss of FGF signaling function, by SU5402 treatment (6-7 µg/ml), genetic disruption of *fgf8* and/or *fgf24*, or ectopic expression of dn-Fgfr1 using *hsp70:dn-fgfr1* transgenic zebrafish, leads to a specific defect in cilium length (8). This discrepancy may arise from variable loss-of-function efficiency due to different inhibitor concentrations, genetic backgrounds or experimental protocols. Regarding the role of *fgf8* in LR asymmetry, severe KV defects including partial or complete loss of KV formation, short cilia, and a reduced number of cilia have been observed in *ace/fgf8* mutants, or knockdown embryos of *fgf8* or *fgf8 effectors* (*ier2* and *fibp1*) (2, 15). In addition, Hong & Dawid have reported that severe KV defects in knockdown embryos of *ier2* and *fibp1* may be associated with disorganization of the DFC cluster (15). These findings also differ from those of Neugebauer et al. (8), but are consistent with our observations that either *ace/fgf8* mutants or *fgf8* morphants display failures of DFC clustering, KV formation and LR asymmetric patterning (Fig. 2F, 3A-C, Fig. S6C, F and Fig. S8C, D). While particular issues remain to be resolved, these results clearly demonstrate that FGF signaling plays important roles in DFC clustering, KV formation, and ciliogenesis.

Role for Cnpy1 in cell signaling

We have revealed a novel insight into the molecular mechanism by which Cnpy1 regulates FGF signaling. Cnpy1 assists Fgfr1 maturation in the ER by binding to ER chaperones and folding enzymes. However, it is noteworthy that Cnpy1 function is not exclusive for FGF signaling. Coimmunoprecipitation experiments have revealed that Cnpy1 not only associates with Fgfr1, but also binds to the Wnt receptor Frizzled or the Nodal receptor ActRII (5). Interestingly, it has been reported that the Wnt signal modulator *duboraya* controls KV ciliogenesis (25) and that the Nodal signal mediator *Ttrap* may participate in DFC cluster formation and ciliogenesis (20), suggesting that the coordinated actions of multiple signaling pathways are required for KV formation. It will therefore be of great interest to establish whether Cnpy1 is essential for the modulation or integration of these pathways.

DFC clustering and adhesion

Contact between DFCs and the overlying surface ectoderm is known to be important for DFCs to migrate toward the vegetal pole (14). Because loss-of-function of FGF signal components (*fgf8* and *cnpy1*) and downstream effectors (*tbx16* and *cdh1*) showed the broken-up DFC clusters but normal migration of these disrupted DFCs to the vegetal pole during gastrulation, FGF signal-dependent cell adhesion may specifically contribute to the interaction between DFCs themselves. However, in these phenotypes, some DFCs remained capable of interacting with others to form small groups of cells, implying that other factor(s) may contribute to DFC clustering. It has been reported that *integrin* αV and *integrin* $\beta 1b$ have a role in DFC clustering (26), and that planar cell polarity (PCP) signaling regulates cell adhesion between DFCs even though knockdown of the signal component *pricle1a* does not lead to a broken-up DFC phenotype (27). Additional experiments to clarify the relationship between FGF signaling and integrins or PCP signaling during DFC cluster formation will be important to understand the entire mechanism underlying DFC cluster formation.

Conclusions

We have discovered the cells (DFCs) in which Cnpy1 functions, and further added a novel insight into the molecular mechanism by which Cnpy1 regulates cell signaling in the ER. We identify an essential signal cascade — ligand, receptor, mediator and downstream effector — which is required for proper cluster formation by progenitor cells. In addition, our findings reveal that progenitor clustering regulated by a positive feedback loop of cell signaling contributes to the formation of a functional organ to establish the left-right asymmetric body plan during vertebrate development.

Materials and Methods

Zebrafish and whole-mount *in situ* hybridization

A wild-type strain (RIKEN-Wako), *Tg[sox17:GFP]* (28) and ace^{ti282a} (2) were used in this study. Single or double-color whole-mount *in situ* hybridization was performed as described previously (29, 30). cDNA fragments of *cdh1*, *cnpy1*, *mlc2a*, *no tail*, *sox32* and *spaw* were used as templates for the antisense probes.

Other Methods

Detailed methods for immunofluorescence analyses, pharmacological experiments and rescue experiments are available at SI Appendix.

Acknowledgements

We are grateful to Thomas N. Sato, Yasukazu Nakahata and Kinichi Nakashima for advice, helpful discussions and critical reading of the manuscript. We also thank Ian Smith for help in preparing the manuscript; Ryutaro Akiyama, Maiko Yokouchi, Takeshi Fujimuro and Naoyuki Tahara for technical assistance; Tatsuro Matsuta for help with statistical analysis; Bruce W. Draper for advice; Kazushige Sakaguchi, Masahiko Hibi and Masatoshi Takeichi for sharing reagents; Kota Yanagitani, Michiko Saito and Kenji Kohno for sharing reagents and discussions; National Bio Resource Project, Zebrafish, Core Institution (NZC) for zebrafish lines *Tg[sox17:GFP] and* *ace*^{ti282a}; ARIAD for AP20187. This work was supported by Grants-in-Aid for Scientific Research on Priority Areas "WAKATE(B)" and "Systems Genomics" from the Ministry of Education, Culture, Sports, Science and Technology (MEXT), Japan; the Nakajima Foundation; and the Global COE Program in NAIST, MEXT, Japan.

References

1. Bottcher, R. T. & Niehrs, C. Fibroblast growth factor signaling during early vertebrate development. *Endocr Rev* **26**, 63-77 (2005).
2. Albertson, R. C. & Yelick, P. C. Roles for fgf8 signaling in left-right patterning of the visceral organs and craniofacial skeleton. *Dev Biol* **283**, 310-21 (2005).
3. Meyers, E. N. & Martin, G. R. Differences in left-right axis pathways in mouse and chick: functions of FGF8 and SHH. *Science* **285**, 403-6 (1999).
4. Tsang, M. & Dawid, I. B. Promotion and attenuation of FGF signaling through the Ras-MAPK pathway. *Sci STKE* **2004**, pe17 (2004).
5. Hirate, Y. & Okamoto, H. Canopy1, a novel regulator of FGF signaling around the midbrain-hindbrain boundary in zebrafish. *Curr Biol* **16**, 421-7 (2006).
6. Amack, J. D. & Yost, H. J. The T box transcription factor no tail in ciliated cells controls zebrafish left-right asymmetry. *Curr Biol* **14**, 685-90 (2004).
7. Amack, J. D., Wang, X. & Yost, H. J. Two T-box genes play independent and cooperative roles to regulate morphogenesis of ciliated Kupffer's vesicle in zebrafish. *Dev Biol* **310**, 196-210 (2007).
8. Neugebauer, J. M., Amack, J. D., Peterson, A. G., Bisgrove, B. W. & Yost, H. J. FGF signalling during embryo development regulates cilia length in diverse epithelia. *Nature* **458**, 651-4 (2009).
9. Hirokawa, N., Tanaka, Y., Okada, Y. & Takeda, S. Nodal flow and the generation of left-right asymmetry. *Cell* **125**, 33-45 (2006).
10. Kramer-Zucker, A. G. et al. Cilia-driven fluid flow in the zebrafish pronephros,

brain and Kupffer's vesicle is required for normal organogenesis. *Development* **132**, 1907-21 (2005).

11. Essner, J. J., Amack, J. D., Nyholm, M. K., Harris, E. B. & Yost, H. J. Kupffer's vesicle is a ciliated organ of asymmetry in the zebrafish embryo that initiates left-right development of the brain, heart and gut. *Development* **132**, 1247-60 (2005).
12. Cooper, M. S. & D'Amico, L. A. A cluster of noninvoluting endocytic cells at the margin of the zebrafish blastoderm marks the site of embryonic shield formation. *Dev Biol* **180**, 184-98 (1996).
13. Melby, A. E., Warga, R. M. & Kimmel, C. B. Specification of cell fates at the dorsal margin of the zebrafish gastrula. *Development* **122**, 2225-37 (1996).
14. Oteiza, P., Koppen, M., Concha, M. L. & Heisenberg, C. P. Origin and shaping of the laterality organ in zebrafish. *Development* **135**, 2807-13 (2008).
15. Hong, S. K. & Dawid, I. B. FGF-dependent left-right asymmetry patterning in zebrafish is mediated by Ier2 and Fibp1. *Proc Natl Acad Sci U S A* **106**, 2230-5 (2009).
16. Sitia, R. & Braakman, I. Quality control in the endoplasmic reticulum protein factory. *Nature* **426**, 891-4 (2003).
17. Wickner, S., Maurizi, M. R. & Gottesman, S. Posttranslational quality control: folding, refolding, and degrading proteins. *Science* **286**, 1888-93 (1999).
18. Pownall, M. E. et al. An inducible system for the study of FGF signalling in early amphibian development. *Dev Biol* **256**, 89-99 (2003).

19. Yamamoto, A. et al. Zebrafish paraxial protocadherin is a downstream target of spadetail involved in morphogenesis of gastrula mesoderm. *Development* **125**, 3389-97 (1998).

20. Esguerra, C. V. et al. Ttrap is an essential modulator of Smad3-dependent Nodal signaling during zebrafish gastrulation and left-right axis determination. *Development* **134**, 4381-93 (2007).

21. Hamada, H., Meno, C., Watanabe, D. & Saijoh, Y. Establishment of vertebrate left-right asymmetry. *Nat Rev Genet* **3**, 103-13 (2002).

22. Raya, A. & Belmonte, J. C. Left-right asymmetry in the vertebrate embryo: from early information to higher-level integration. *Nat Rev Genet* **7**, 283-93 (2006).

23. Rohner, N. et al. Duplication of fgfr1 permits Fgf signaling to serve as a target for selection during domestication. *Curr Biol* **19**, 1642-7 (2009).

24. Eggenschwiler, J. T. & Anderson, K. V. Cilia and developmental signaling. *Annu Rev Cell Dev Biol* **23**, 345-73 (2007).

25. Oishi, I., Kawakami, Y., Raya, A., Callol-Massot, C. & Izpisua Belmonte, J. C. Regulation of primary cilia formation and left-right patterning in zebrafish by a noncanonical Wnt signaling mediator, duboraya. *Nat Genet* **38**, 1316-22 (2006).

26. Ablooglu, A. J., Tkachenko, E., Kang, J. & Shattil, S. J. Integrin alphaV is necessary for gastrulation movements that regulate vertebrate body asymmetry. *Development* **137**, 3449-58 (2010).

27. Oteiza, P. et al. Planar cell polarity signalling regulates cell adhesion properties in progenitors of the zebrafish laterality organ. *Development* **137**, 3459-68

(2010).

28. Mizoguchi, T., Verkade, H., Heath, J. K., Kuroiwa, A. & Kikuchi, Y. Sdf1/Cxcr4 signaling controls the dorsal migration of endodermal cells during zebrafish gastrulation. *Development* **135**, 2521-9 (2008).

29. Matsui, T. et al. Noncanonical Wnt signaling regulates midline convergence of organ primordia during zebrafish development. *Genes Dev* **19**, 164-75 (2005).

30. Hauptmann, G. & Gerster, T. Two-color whole-mount in situ hybridization to vertebrate and Drosophila embryos. *Trends Genet* **10**, 266 (1994).

Figure Legends

Figure 1. Cnpy1 within DFCs regulates DFC clustering during zebrafish gastrulation. (A, B) dp-Erk staining in DFC$^{\text{control-MO}}$-injected (A) or DFC$^{cnpy1\text{-MO}}$-injected (B) *Tg[sox17:GFP]* embryos at 60% epiboly stage. Scale bar: 20 µm. dp-Erk signals (red) were down-regulated in GFP-positive DFCs (green). (C, D) *cnpy1* (purple) and *sox32* (red) expression in DMSO-treated (C) or SU5402-treated (D) embryos at 60% epiboly stage. Scale bar: 200 µm. SU5402 reduced *cnpy1* expression in DFCs. Dotted lines in A-D mark the outlines of DFC populations. (E-J) *sox32* expression in DFC$^{\text{control-MO}}$ (E), DFC$^{cnpy1\text{-MO}}$ (F), yolk$^{\text{control-MO}}$ (G), yolk$^{cnpy1\text{-MO}}$ (H), DFC$^{cnpy1\text{-MO+mRFP}}$ (I) or DFC$^{cnpy1\text{-MO+Cnpy1}}$ (J) embryos at 70% epiboly stage. Dorsal view, anterior to the top. Scale bar: 200 µm. (E'-J') Higher-magnification images highlight DFCs. (K) Percentages of normal (clustered) or broken-up DFCs were scored using the *sox32* expression pattern in uninjected (n = 68), *cnpy1*-MO (n = 77), DFC$^{\text{control-MO}}$ (n = 61), DFC$^{cnpy1\text{-MO}}$ (n = 78), yolk$^{\text{control-MO}}$ (n = 56), yolk$^{cnpy1\text{-MO}}$ (n = 62) DFC$^{cnpy1\text{-MO+mRFP}}$ (n = 119) or DFC$^{cnpy1\text{-MO+Cnpy1}}$ (n = 123) embryos. Statistically significant ($P < 0.05$) differences could be seen in uninjected versus *cnpy1*-MO ($P = 5.66 \times 10^{-8}$), DFC$^{\text{control-MO}}$ versus DFC$^{cnpy1\text{-MO}}$ ($P = 3.31 \times 10^{-5}$) and DFC$^{cnpy1\text{-MO+mRFP}}$ versus DFC$^{cnpy1\text{-MO+Cnpy1}}$ ($P = 0.00174$), while no difference was seen in uninjected versus DFC$^{\text{control-MO}}$ ($P = 0.707$), uninjected versus yolk$^{\text{control-MO}}$ ($P = 1.000$), DFC$^{\text{control-MO}}$ versus yolk$^{\text{control-MO}}$ ($P = 0.439$) or yolk$^{\text{control-MO}}$ versus yolk$^{cnpy1\text{-MO}}$ ($P = 0.667$).

Figure 2. Cnpy1 function within DFCs is essential for ciliogenesis and LR

patterning. (A, B) A-tubulin (green) and nucleus (red) staining in uninjected (A) or DFC$^{\textit{cnpy1}\text{-MO}}$-injected (B) embryos at the 6-somite stage. Vegetal pole view. Scale bar: 20 µm. (A’, B’) X-Z view around the KV. Lumen formation was not completed in DFC$^{\textit{cnpy1}\text{-MO}}$-injected embryos (B’). (C) Number (red) or length (blue) of KV primary cilia in uninjected (n = 10 or 49), DFC$^{\textit{cnpy1}\text{-MO}}$ (n = 10 or 48), yolk$^{\text{control-MO}}$ (n = 11 or 77), yolk$^{\textit{cnpy1}\text{-MO}}$ (n = 11 or 58), DFC$^{\textit{cnpy1}\text{-MO+mRFP}}$ (n = 10 or 61) or DFC$^{\textit{cnpy1}\text{-MO+Cnpy1}}$ (n = 11 or 85) embryos. Error bars show s.e.m. Statistically significant ($P < 0.05$) differences could be seen in uninjected versus DFC$^{\textit{cnpy1}\text{-MO}}$ ($P = 1.08 \times 10^{-7}$ or 5.85×10^{-14}) and DFC$^{\textit{cnpy1}\text{-MO+mRFP}}$ versus DFC$^{\textit{cnpy1}\text{-MO+Cnpy1}}$ ($P = 7.72 \times 10^{-4}$ or 1.07×10^{-14}), while no difference was seen between uninjected and yolk$^{\text{control-MO}}$ ($P = 0.261$ or 0.439) or yolk$^{\text{control-MO}}$ and yolk$^{\textit{cnpy1}\text{-MO}}$ ($P = 0.546$ or 0.609). (D, E) Representative images of *mlc2a* expression demonstrating normal-looping (uninjected; D) or reversed-looping (*cnpy1*-MO; E) of the heart in embryos at the high pec stage. Ventral view, anterior to the top. A: atrium; V: ventricle. (F) Percentages of normal-looping, reversed-looping, no-looping or cardia bifida of the heart in uninjected (n = 164), control-MO (n = 118), *cnpy1*-MO (n = 119), *fgf8*-MO (n = 65), DFC$^{\text{control-MO}}$ (n = 95), DFC$^{\textit{cnpy1}\text{-MO}}$ (n = 146), DFC$^{\textit{cdh1}\text{-MO}}$ (n = 106), yolk$^{\text{control-MO}}$ (n = 96), yolk$^{\textit{cnpy1}\text{-MO}}$ (n = 94), DFC$^{\textit{cnpy1}\text{-MO+mRFP}}$ (n = 136) and DFC$^{\textit{cnpy1}\text{-MO+Cnpy1}}$ (n = 165) embryos. Statistically significant ($P < 0.05$) differences could be seen in uninjected versus *cnpy1*-MO ($P < 2.2 \times 10^{-16}$), DFC$^{\text{control-MO}}$ versus DFC$^{\textit{cnpy1}\text{-MO}}$ ($P = 6.53 \times 10^{-13}$) and DFC$^{\textit{cnpy1}\text{-MO+mRFP}}$ versus DFC$^{\textit{cnpy1}\text{-MO+Cnpy1}}$ ($P = 0.0294$), but not in uninjected versus DFC$^{\text{control-MO}}$ ($P = 0.674$), uninjected versus yolk$^{\text{control-MO}}$ ($P = 0.08$), DFC$^{\text{control-MO}}$ versus yolk$^{\text{control-MO}}$ ($P = 0.328$) or yolk$^{\text{control-MO}}$

versus yolk$^{\textit{cnpy1}\text{-MO}}$ ($P = 0.497$).

Figure 3. FGF signaling plays crucial roles in DFC clustering and KV ciliogenesis to control left-right patterning in the body. (A, B) *sox32* (A) or *no tail* (B) expression in *fgf8*-MO-injected embryos. Dorsal view, anterior to the top. Scale bar: 200 μm. (A', B') Higher-magnification images highlight DFCs. The white dotted lines mark the boundary between DFCs and the blastoderm margin (B', D, E). (C) Percentages of normal or broken-up DFCs were scored using the *sox32* or *no tail* expression patterns in uninjected (n = 68 or 89) or *fgf8*-MO (n = 61 or 69) embryos. Statistically significant ($P < 0.05$) differences could be seen in uninjected versus *fgf8*-MO ($P = 1.76 \times 10^{-6}$ or 1.08×10^{-10}). (D-K) Transient activation of FGF signaling restored the broken-up DFC phenotype (D-F), ciliogenesis (G-J) and cardiac laterality (K) in DFC$^{\textit{cnpy1}\text{-MO}}$ embryos. (D, E) Expression of *no tail* in DFC$^{\textit{cnpy1}\text{-MO+iFGFR1}}$ embryos treated with ethanol (D) or AP20187 (E). (F) Percentages of broken-up DFC phenotype in ethanol- (n = 84) or AP20187-treated (n = 93) DFC$^{\textit{cnpy1}\text{-MO+iFGFR1}}$ embryos. The conditional activation of Fgfr1 after treatment with AP20187 significantly decreased the broken-up DFC phenotype (67%; $P = 2.89 \times 10^{-4}$). (G-J) A-tubulin (green) staining in ethanol- (G) or AP20187-treated (H) DFC$^{\textit{cnpy1}\text{-MO+iFGFR1}}$ embryos at the 6-somite stage. Scale bar: 20 μm. (I, J) Number (I) or length (J) of KV primary cilia in ethanol-treated DFC$^{\textit{cnpy1}\text{-MO+iFGFR1}}$ (n = 9 or 36) or AP20187-treated DFC$^{\textit{cnpy1}\text{-MO+iFGFR1}}$ (n = 8 or 34) embryos at the 6-somite stage. Error bars show s.e.m. Statistically significant ($P < 0.05$) differences could be seen in ethanol-treated versus AP20187-treated DFC$^{\textit{cnpy1}\text{-MO+iFGFR1}}$

($P = 9.23 \times 10^{-3}$ or 7.77×10^{-3}). (K) Percentages of cardiac laterality defect in ethanol- (n = 89) or AP20187-treated (n = 102) DFC$^{\textit{cnpy1}\text{-MO+iFGFR1}}$ embryos. The conditional activation of Fgfr1 after treatment with AP20187 alleviated the cardiac laterality defect (48%; $P = 2.89 \times 10^{-4}$).

Figure 4. Cnpy1 enhances FGF receptor maturation within the ER (A, B) Fgfr1 N-glycosylation level was examined by PNGase F (lanes 2, 6) or endo H (lanes 3, 7) treatment. Lanes 1-3: mock control cells; 5-7: Cnpy1-overexpressing cells. Fgfr1 and Cnpy1 were tagged with HA and Flag, respectively (for details, see Material and Methods in SI Appendix). The top panel indicates the glycosylation levels of Fgfr1, and the bottom panel shows expression of Cnpy1 protein. (B) Ratio of glycosylated (black) and non-glycosylated (white) forms of Fgfr1. The amount of the endo H-resistant mature form of Fgfr1 in Cnpy1-overexpressing cells (lane 7) was twice that in mock control cells (lane 3).

Figure 5. A Cnpy1-mediated FGF positive loop regulates cell adhesion through the control of *cdh1* expression. (A, B) *cdh1* (purple) and *sox32* (red) expression in DFC$^{\text{control-MO}}$ (A) or DFC$^{\textit{cnpy1}\text{-MO}}$ (B) embryos at 65% epiboly stage. (C, D) *tbx16* (purple) and *sox32* (red) expression in DFC$^{\text{control-MO}}$ (C) or DFC$^{\textit{cnpy1}\text{-MO}}$ (D) embryos at 65% epiboly stage. Dotted lines in A-D mark the outlines of DFC populations. Scale bar: 200 μm. Expression of *cdh1* or *tbx16* was down-regulated in sparse DFC populations marked by *sox32*. (E-G) Ectopic expression of Cdh1 rescued the broken-up

DFC phenotype in DFC$^{\textit{cnpy1}\text{-MO}}$ embryos. (E, F) Expression of *sox32* in DFC$^{\textit{cnpy1}\text{-MO + mRFP}}$ (E) or DFC$^{\textit{cnpy1}\text{-MO + Cdh1}}$ (F) embryos at 80% epiboly. Scale bar: 200 µm. (G) Percentage of broken-up DFC phenotype in mRFP- (n = 82) or Cdh1-overexpressing (n = 103) DFC$^{\textit{cnpy1}\text{-MO}}$ embryos. Overexpression of Cdh1 rescued the broken-up DFC phenotype in DFC$^{\textit{cnpy1}\text{-MO}}$ embryos (60%; $P = 4.2 \times 10^{-4}$). (H) Diagram illustrating the FGF-dependent cell-cell communication control mechanisms of the forerunner cell cluster during early development. The model depicts the activation of intracellular FGF signaling via binding of Fgf8 ligands and Fgfr1 on the cell surface of two adjacent DFCs (blue ovals). The amplified FGF signal, through Cnpy1-mediated maturation of Fgfr1 within DFCs, subsequently activates the expression of *tbx16* and *cdh1* to organize forerunner cells as a cluster.

Matsui_Figure1

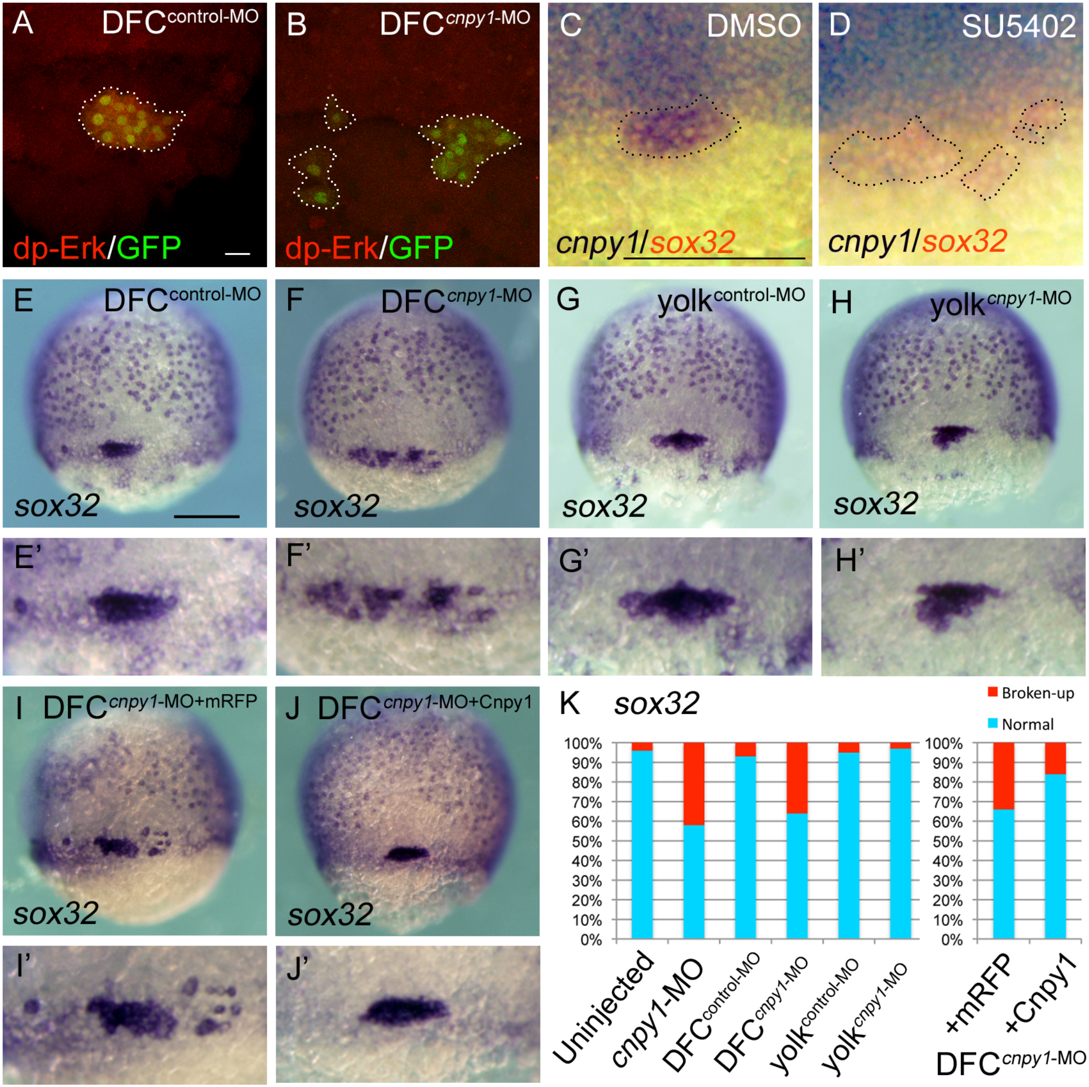
A DFC$^{\text{control-MO}}$
dp-Erk/GFP
B DFC$^{\textit{cnpy1}\text{-MO}}$
dp-Erk/GFP
C DMSO
cnpy1/sox32
D SU5402
cnpy1/sox32
E DFC$^{\text{control-MO}}$
sox32
F DFC$^{\textit{cnpy1}\text{-MO}}$
sox32
G yolk$^{\text{control-MO}}$
sox32
H yolk$^{\textit{cnpy1}\text{-MO}}$
sox32
E'
F'
G'
H'
I DFC$^{\textit{cnpy1}\text{-MO+mRFP}}$
sox32
J DFC$^{\textit{cnpy1}\text{-MO+Cnpy1}}$
sox32
I'
J'
K sox32
Broken-up
Normal
100%
90%
80%
70%
60%
50%
40%
30%
20%
10%
0%
Uninjected
cnpy1-MO
DFC$^{\text{control-MO}}$
DFC$^{\textit{cnpy1}\text{-MO}}$
yolk$^{\text{control-MO}}$
yolk$^{\textit{cnpy1}\text{-MO}}$
+mRFP
+Cnpy1
DFC$^{\textit{cnpy1}\text{-MO}}$

Matsui_Figure 2

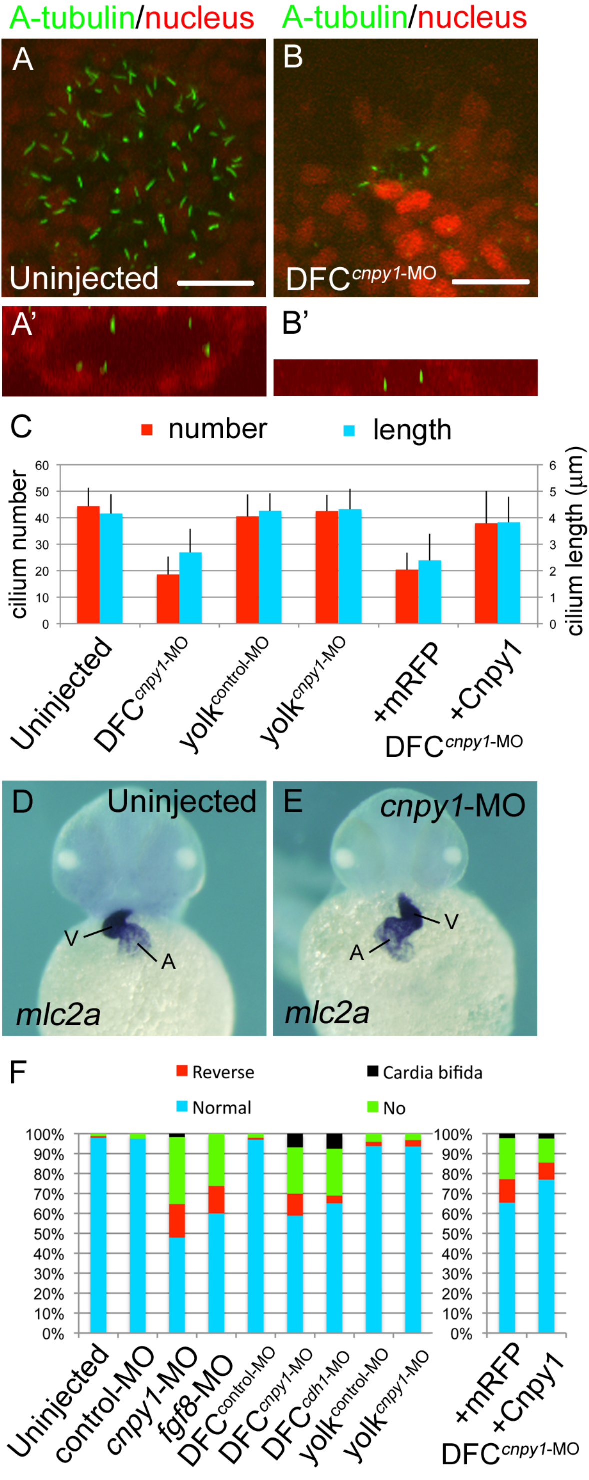

Matsui_Figure 3

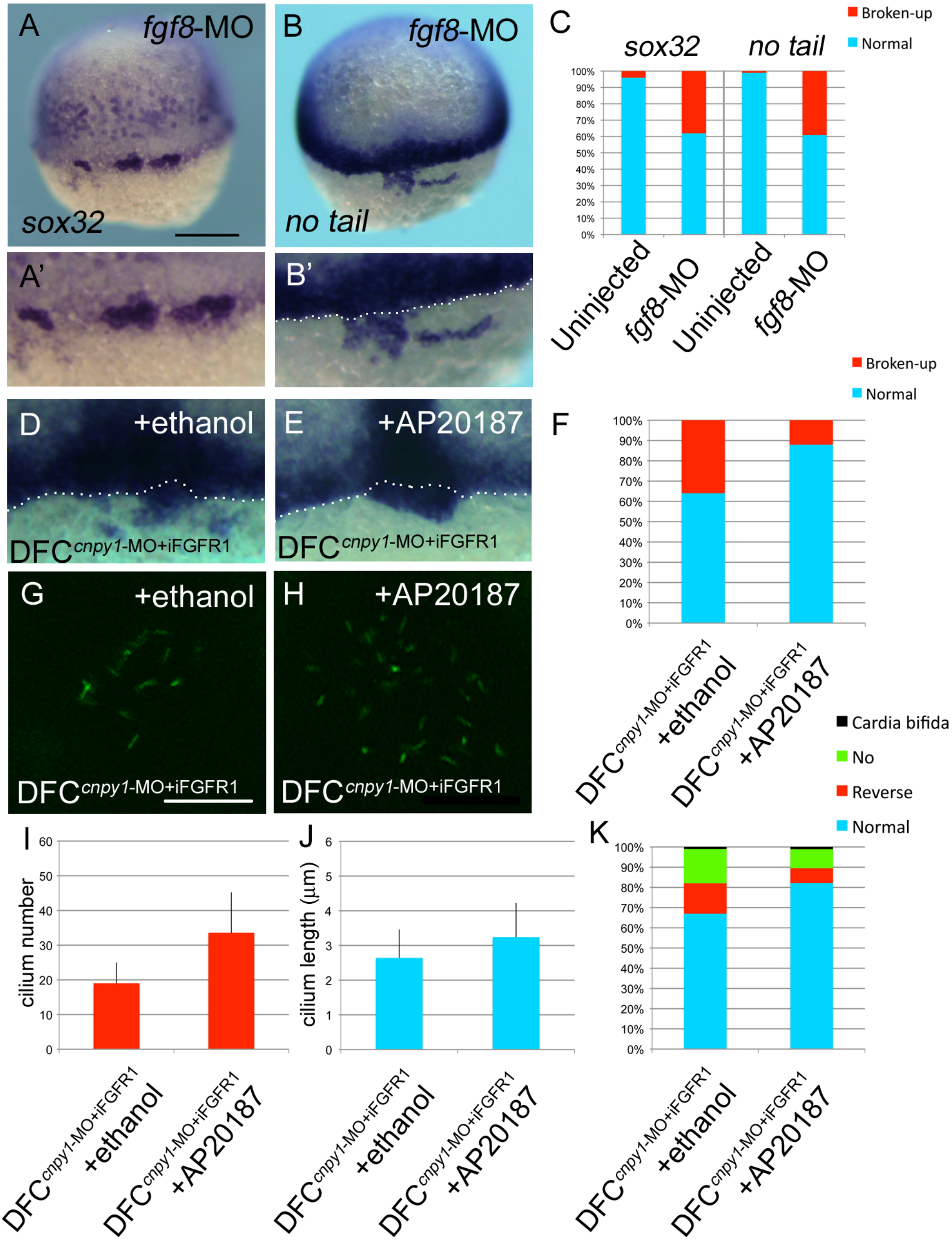

Matsui_Figure 4

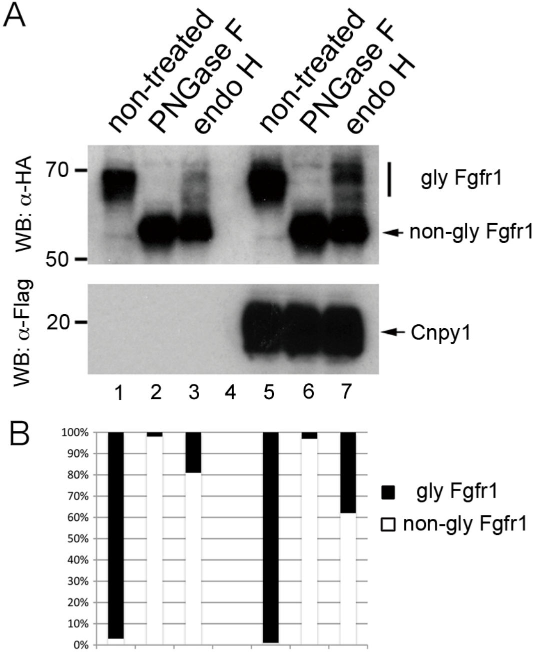

Matsui_Figure5

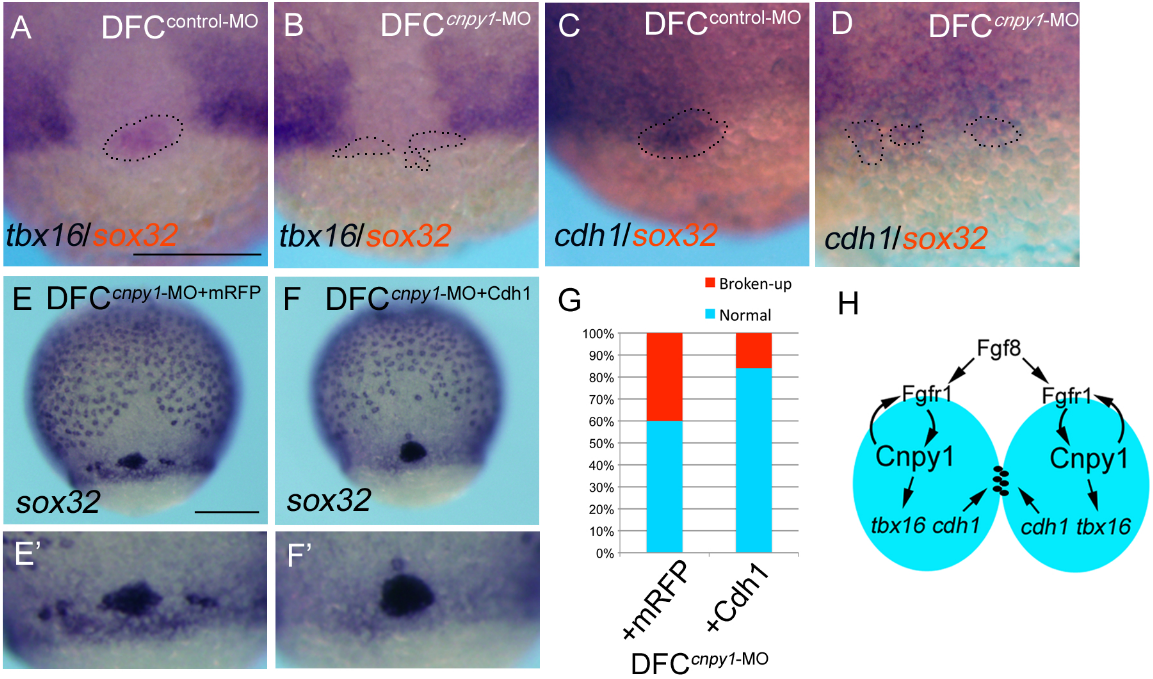
A
DFC control-MO
tbx16/sox32
B
DFC cnpy1-MO
tbx16/sox32
C
DFC control-MO
cdh1/sox32
D
DFC cnpy1-MO
cdh1/sox32
E
DFC cnpy1-MO+mRFP
sox32
F
DFC cnpy1-MO+Cdh1
sox32
E'
F'
G
Broken-up
Normal
100%
90%
80%
70%
60%
50%
40%
30%
20%
10%
0%
+mRFP
+Cdh1
DFC cnpy1-MO
H
Fgf8
Fgfr1
Fgfr1
Cnpy1
Cnpy1
tbx16 cdh1
cdh1 tbx16